# Effects of Ni on the microstructure, hot tear and mechanical properties of AleZneMgeCu alloys under as-cast condition

Fuchu Liu [a, b], Xiangzhen Zhu [a], Shouxun Ji [a, *]

[a] Brunel Centre for Advanced Solidification Technology (BCAST), Institute of Materials and Manufacturing, Brunel University London, Uxbridge, Middlesex, UB8 3PH, United Kingdom [b] State Key Laboratory of Materials Processing and Die & Mould Technology, Huazhong University of Science and Technology, Wuhan, 430074, China

Abstract

The effects of Ni on the phases, microstructural evolution, hot tear susceptibility and mechanical properties of Ale6Zn-1.4Mg-1.2Cu alloys fabricated by gravity casting were investigated using X-ray diffraction (XRD), scanning electronic microscopy (SEM), optical microscopy, the N-Tec Hot tear and tensile test. The calculation of phase diagrams (CALPHAD) modelling was also conducted to understand the phase formation of the experimental alloys. The results showed that the secondary phases (including h-MgZn2,SeAl2CuMg and Al3Ni) are mainly distributed at grain boundary, while round SeAl2CuMg particles are also found in a-Al matrix. Ni only exists as Al3Ni with different morphologies and its number density ascends with the increase of Ni content in alloys, which also significantly improves the hot tear resistance. As a result, the increased Ni in the alloys remarkably improves the ultimate tensile and yield strength, while the elongation increases when Ni < 0.6 wt% followed by decreases when Ni > 0.6 wt%. 

## 1. Introduction

The development in aerospace and automobile industry demands the continuous improvement of aluminum alloys for better mechanical performance [1e5]. AleZneMgeCu (7xxxx) alloys have been widely used in wrought products [4,5] to offer high specific strength in light weight structure. In recent years, the interests in developing castable AleZneMgeCu alloys for shaped casting is increased [6e10], targeting to reduce the manufacturing cost but maintain the high-strength in components. However, one of the problems is the high tendency to form hot tear during solidification [9e11]. Once hot tear occurs, the casting components should be repaired or even discarded, which significantly limits the application of AleZneMgeCu alloys in the manufacturing of shaped castings.

In order to overcome the hot tear problem and tailor the mechanical properties of AleZneMgeCu cast alloys, the efforts have mainly focused on using special casting techniques [12e22] and developing novel aluminum alloys [23e29]. The special casting techniques including powder metallurgy [12], semi-solid metal processing [13e16], rapid solidification [17], spray deposition [18e20] and electromagnetic casting [21,22], have been

used to achieve the near-net shape casting of AleZneMgeCu alloys. However, these casting techniques are only effective in specific components, but not very applicable in massive manufacturing of components with complex shapes, in particular when combining the consideration of manufacturing cost.

In reality, the development through modifying the elemental constituents is a cost-effective, simple and proved approach in application. It is easy to apply in conventional foundry practice without significant changes in processing equipment and procedures. Previous studies confirmed that the modification of main alloying elements and their contents had complex and/or even contradictory effects on the hot tear tendency of AleZneMgeCu alloys [11,23,24]. Krajewski [25] and S. Shin et al. [26] pointed that extra high Zn level (>20 wt%) could effectively suppress the formation of hot tear during solidification, however, the high density induced by high Zn is not favoured for light-weight requirement. On the other side, grain refinement using AleTi or AleTieB master alloys has been extensively studied to reduce hot tear and simultaneously increase the strength and elongation of cast aluminium alloys [27e29].J. Shin et al. [29] found that the addtion of Ti have a positive effect on the reduction of hot tear susceptibility. However, Warrington et al. [24] found that the addition of excessive grain refiner lead to the increase of hot tear susceptibility because of the

Table 1
Chemical compositions of AleZneMgeCu-xNi alloys analyzed by OES (wt.%).

| Alloy[a] | Zn | Mg | Cu | Ni | Ti | Fe | Others | Al |
|---|---|---|---|---|---|---|---|---|
| AleZneMgeCueNi | 6 ± 0.11 | 1.4 ± 0.06 | 1.2 ± 0.05 | Varied | 0.02 ± 0.01 | 0.08 ± 0.01 | <0.05 | Bal. |

a Actual Ni contents were measured to be 0.03, 0.34, 0.63, 0.94, 1.25, 1.67, 2.68, 3.69 and 4.71, respectively.

formation of equiaxed-cellular grains in alloys. Moreover, in order to decrease the hot tear susceptibility of cast AleZn alloys, other elements were also studied [29]. J. Shin et al. [29] claimed that Si could eliminate the hot tear when Si content is up to 3 wt% in the as-cast Ale6Zne1Mge3Si-0.1Zr-0.1Ti alloy. Unfortunately, the addtion of Si remarkably worsen the elongation. Therefore, an applicable solution to decrease the hot tear tendency and maintain or improve the mechanical properties of AleZn based alloys is urgently needed. Recently, Ni was found as a potential element capable of achieving these goals. The addition of Ni in Al alloys can increase the strength at room or elevated temperatures [30e36], which have been widely confirmed in Al-Si [30e33], AleMgeSieMn [34], Al-Si-Cu-Mg [35] and AleZneMgeCu [36] alloys. Meanwhile, Belov et al. [37e39] analyzed the equilibrium phase diagram of AleZneMg-(Cu)eNi alloys using Thermal-Calo software, and found that Ni only exists in the form of Al þ Al3Ni eutectics. Generally, the increase of eutectics is helpful to supress the formation of hot tear in cast alloys. It is speculated that the Ni addition can further increase the effectiveness of strengthening in AleZn based alloys when the hot tear resistance was improved. However, there is no experimental evidence supporting these expectations up to now.

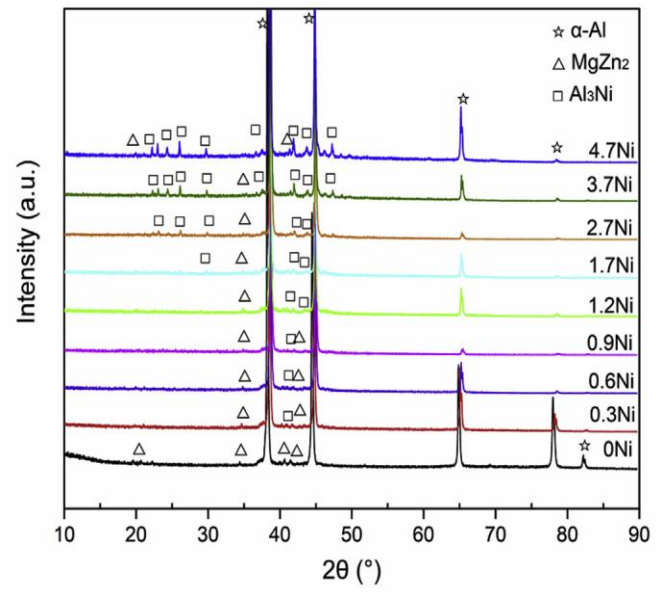


Fig.1.XRDpatternsoftheAleZneMgeCueNialloysunderas-castcondition.

Therefore, in this paper, it is aimed to study the effect of Ni on the microstructure, hot tear and mechanical properties of AleZneMgeCu alloys. A series of AleZneMgeCu alloys with different Ni contents were prepared by gravity casting. The hot tear susceptibility was measured, and the phase formation and microstructure were analyzed in association with the mechanical properties. The phase formation was also studied through the calculation of phase diagrams (CALPHAD) modelling of multi-component AleZneMgeCueNi system. The mechanism of improving the hot tear resistance was analyzed by the theoretical calculation of solid fractions and surface morphology. The relationship between microstructure and mechanical properties is also discussed in the experimental alloys.

## 2. Experimental

The alloys with a nominal composition of Ale6Zn-1.4Mg-1.2CuxNi (x ¼ 0, 0.3, 0.6, 0.9, 1.2, 1.7, 2.7, 3.7 and 4.7, hereafter denoted AleZneMgeCu-xNi) were prepared by melting pure Al, Zn, Mg, Cu, and Al-20 wt% Ni master alloy (all compositions reported in this paper are in wt.% unless otherwise clarified). During alloy preparation, firstly, the pure Al and Cu, Al-20 wt% Ni master alloy were melted in a 12-kg clay-graphite crucible coated with boron nitride using an electric resistance furnace at 780 ± 5 $^{0}$C. Secondly, pure Zn and Mg were added into the melt, followed by gentle stirring the melt, Zn and Mg was over added by 5 wt% respectively for compensating the burning lost during melting. After 30 min of homogenization at 750 $^{0}$C, the melt was degassed using high purity argon input through a rotary impeller at a speed of 300 rpm for 6 min. After degassing, 0.1 wt% Ale5Tie1B master alloy was added into the melt for grain refinement, and then the melt was held at 720 $^{0}$C for 30 min before casting. During casting, a metal mold to make two tensile samples was used, which is made according to ASTM Be108 for the details of gating system and casting structure [40,41]. The mold was coated with boron nitride and preheated up to 400 $^{0}$C. The pouring temperature was controlled at 720 $^{0}$C. All casting samples were kept under ambient condition for 3 days before the tensile testing.

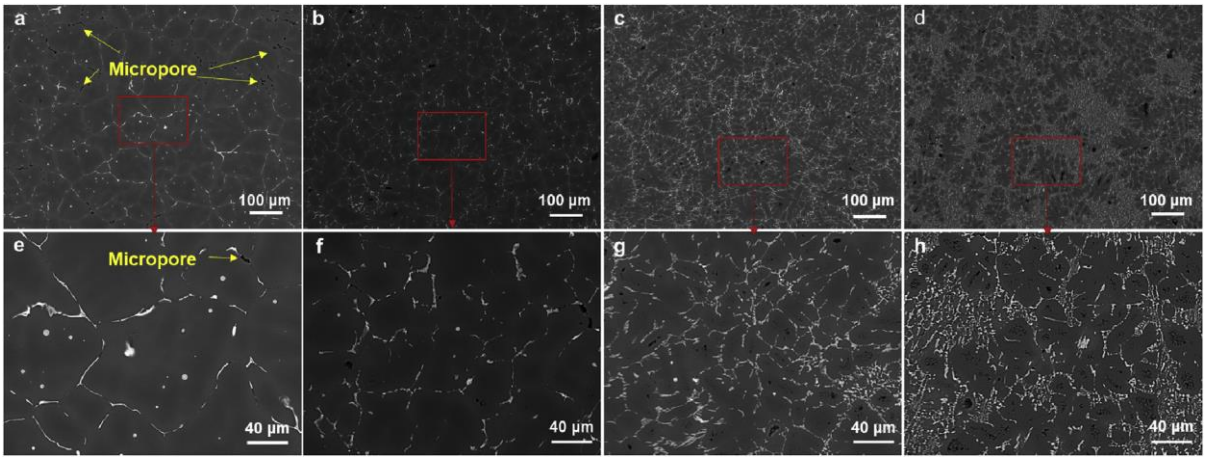


Fig. 2. Backscattered SEM images showing the as-cast microstructure of AleZneMgeCueNi alloys, (a,e) 0Ni, (b,f) 0.6Ni, (c,g)2.7Ni and (d,h) 4.7Ni.

The mushroom samples for the composition analysis were obtained by pouring the melt into a permanent mold preheated at 200 $^{0}$C 3 mm thick of materials at the bottom of the mushroom samples were machined off before applying the composition analysis. The chemical compositions were measured using Foundry-Master Pro optical emission spectrometer (OES) with testing five sparks. The average value was taken as the results, listed in Table 1.

The hot tear susceptibility (HTS) was measured by using an N-Tec Hot tear test mold [42,43], which consists of five 'dog bone' sections with different lengths, constrained at each end with a hot spot along their length. The HTS test mold was coated with boron nitride and preheated to 250 $^{0}$C. HTS values were calculated using equation (1). Where Li is the length indexing of the dog bone where the crack appeared and Ci is the severity indexing of the crack, and their indexing values can be found in Refs. [42,43].

Tensile testing was performed at room temperature (25 $^{0}$C) according to ASTM B557 M standard using an Instron 5500 Universal Electromechanical Testing Systems equipped with Bluehill software and a ±50 kN load cell. The elongation of samples was measured using an extensometer with the gauge length of 50 mm, and the ramp rate was selected as 1 mm/min during tensile tests. At least five samples were measured to obtain the average value of ultimate tensile strength (UTS), yield strength (YS) and elongation (El).

The X-ray diffraction (XRD) patterns of the samples were examined using the D8 Advance X-Ray Diffractometer equipped with Cu Ka radiation in the range of 10e90$^{0}$ at a scanning speed of 1$^{0}$/min. The specimens for microstructural characterization were cut from the middle of F10 mm round tensile bars and prepared using a standard procedure [44]. The Keller agent (1 vol% HF, 1.5 vol % HCl, 2.5 vol% HNO3 and 95 vol% H2O) was used for chemical

etching. The microstructure was examined utilizing a LEO 1455VP or Zeiss SUPRA 35VP field emission scanning electron microscope

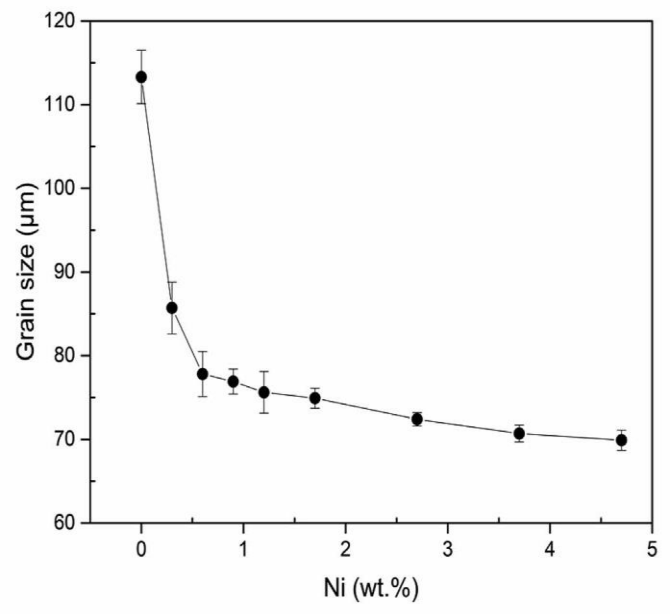


Fig.4.EffectofNicontentontheaveragesizeofa-Algrainsintheas-castAleZneMgeCueNialloys.

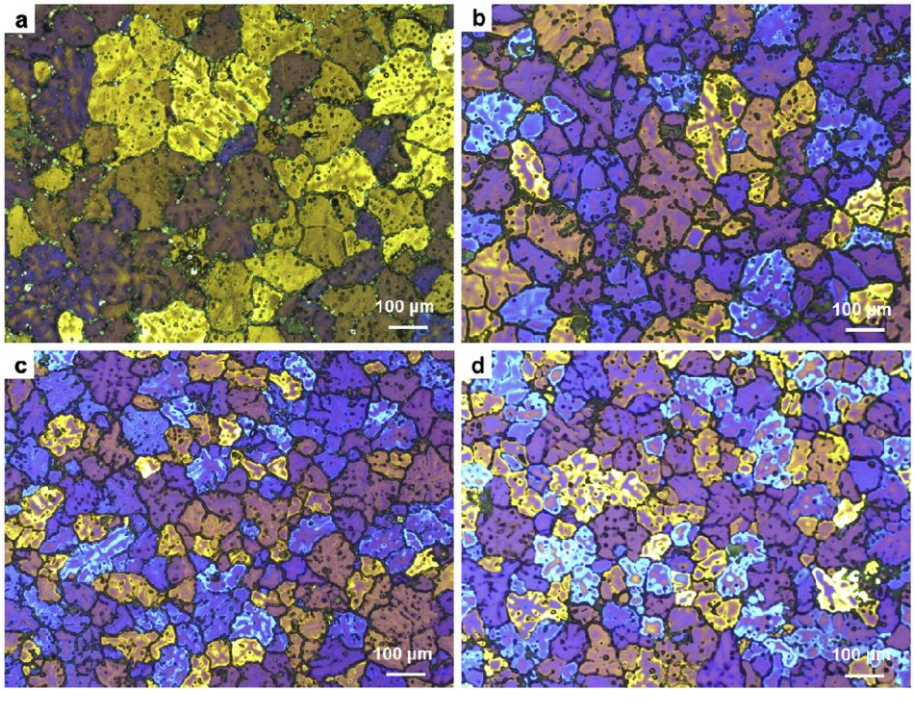

Fig. 3. Polarized images showing the as-cast microstructure of AleZneMgeCueNi alloys, (a) 0Ni, (b) 0.3Ni, (c) 0.6Ni and (d) 0.9Ni.

(SEM) equipped with energy dispersive X-ray spectroscopy (EDS) working at an accelerating voltage of 20 kV. The microstructure of hot tear and tensile fracture surface was probed instantaneously by SEM operated at the secondary electron (SE) mode and backscatter electron mode (BSE). The calculation of the average grain size was conducted using Image-J software after anodized the polished surface of each sample in Barker reagent (3 vol% HBF4 aqueous solution) operated at 20 V for 90s.

## 3. Results

### 3.1. Phase formation and microstructural evolution

Fig. 1 shows the XRD patterns of the as-cast AleZneMgeCu-xNi alloys (denoted as xNi hereafter). The peaks of a-Al and MgZn2 phases were always obvious in the samples. The Al3Ni phase was also observed in the Ni-containing alloys and the peak intensity were increased when Ni content was increased, indicating that the amount of Al3Ni phase was increased.

To understand the phases and microstructure of AleZneMgeCu-xNi alloys, the representative backscattered SEM images showing the as-cast microstructure of AleZneMgeCueNi alloys are shown in Fig. 2. All the experimental alloys included gray primary a-Al grains with equiaxed morphology and bright inter-metallic phases with different shapes including

rod-like, round and agglomerated particles. It was also noticed that the Ni-containing alloys had a much smaller a-Al grain size. The polarized images showing the microstructure of as-cast AleZneMgeCueNi alloys are shown in Fig. 3 and the average size of a-Al grain are depicted in Fig. 4 as a function of Ni content. Clearly, when the Ni content was increased, the average size of a-Al grains was reduced from 113 mm (0Ni) to 77 mm (0.6Ni), and graduately stablised at 70 mm for the increased Ni content.

The intermetallic phases and the corresponding EDS analysis results are shown in Fig. 5. It is seen that the alloy without Ni consisted of a-Al phase, h-MgZn2 phase and SeAl2CuMg phase under as-cast condition. From the EDS analysis, the primary a-Al phase was enriched by 2.29 at.% Zn, 2.11 at.% Mg and 0.67 at.% Cu, which is agreed with others' results [6,7,23]. The irregular h-MgZn2 phase was distributed at grain boundaries. The round SeAl2CuMg phase was distributed mainly in the a-Al matrix from the alloy containing increased Ni content. The EDS results shown in Fig. 5 indicated that SeAl2CuMg phase (marked at C) contained much higher Zn (8.71 at.%) than Al matrix (2.29 at.%) had. When Ni was increased in the alloys, Al3Ni phase was formed while other phases had no obvious change. When Ni content was less than 0.6 wt%, Al3Ni had a morphology of fine dots or irregular strips, which were usually associated with irregular h-MgZn2 phase in the eutectic areas, as shown in Figs. 5b and 6a. The EDS results shown in Fig. 5 confirmed that Al3Ni phase did not contain other elements.

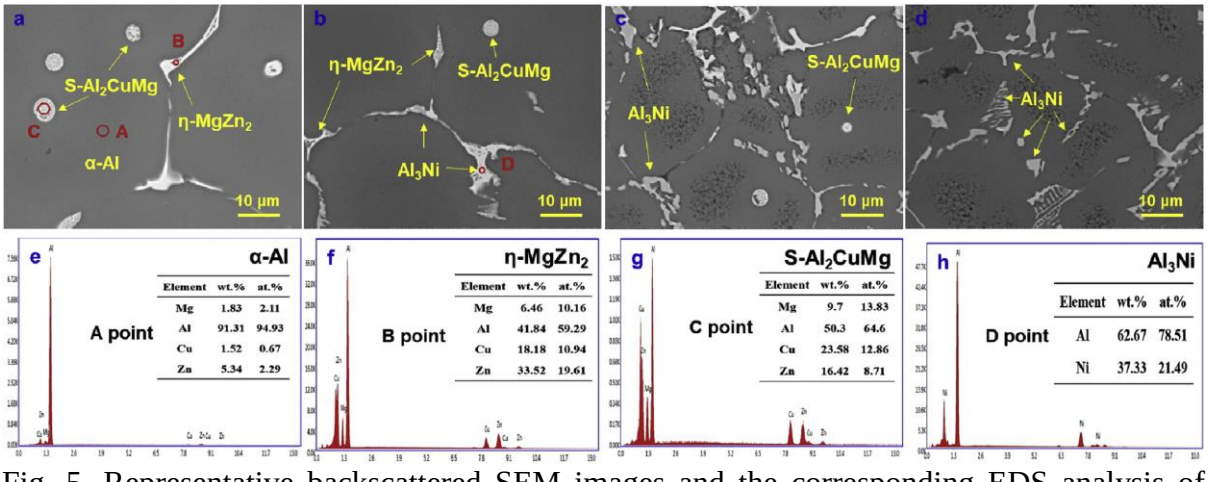

Fig. 5. Representative backscattered SEM images and the corresponding EDS analysis of different phases in the as-cast AleZneMgeCueNi alloys, (a) 0Ni, (b) 0.6Ni, (c) 2.7Ni, (d) 4.7Ni, (e)A point, (f)B point, (g)C point and (h)D point.

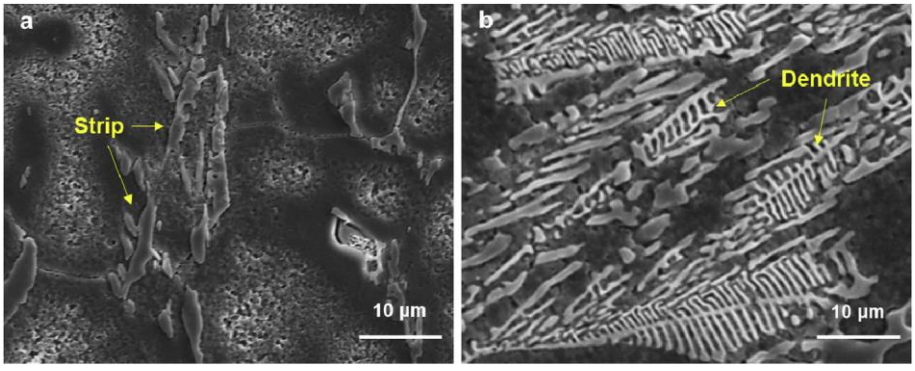

Fig. 6. Typical morphologies of eutectic Al3Ni phase, (a) strip and (b) dendrite.

Therefore, Ni did not form phases with Zn, Mg and Cu. When Ni content was more than 0.9 wt%, the Al3Ni phase became coarse but still showed a strip-like morphology. However, the Al3Ni phase showed a long dendritic morphology (Fig. 6b) with a length of about 35 mm in the alloy containing 4.7 wt% Ni. This morphology has not been reported in literatures. However, the widely reported rod-like morphology of Al3Ni phase was also not observed in the present work [45,46].

3.2. Hot tear susceptibility

Fig. 7 shows the calculated HTS indexes according to equation (1) and the castings for testing hot tear before demolding. It is clear that the HTS values was decreased as the Ni content was raised. The alloy without Ni had the highest HTS value of 17.36 and three dog bones were observed with cracks. When the Ni content was increased, the HTS values were gradually decreased from 12.37 in the alloy with 0.3 wt%Ni to 9.23 in the alloy with 0.6 wt%Ni and 5.44 in the alloy with 0.9 wt%Ni. When the Ni content was greater than 1.2 wt%, the HTS values were dropped to 0, meaning that there was no tendency to hot tear. The results clearly confirmed that Ni could effectively eliminate the formation of hot tear in the experimental AleZneMgeCueNi alloys.

3.3. Mechanical properties under as-cast condition

Fig. 8 depicts the mechanical properties of the as-cast AleZneMgeCueNi alloys at room temperature. It is seen three different changes for the ultimate tensile strength (UTS), yield strength (YS) and elongation (El). When Ni was added at a level from 0 to 0.6 wt%, the yield strength was increased from 201.3 MPa to 221.7 MPa, and the elongation was also increased from 0.99% to 1.86%. When Ni was increased from 0.6 to 0.9 wt%, the yield strength was increased to 231.3 MPa, but the elongation was decreased to 1.49%. When Ni content was further increased from 0.9 wt% to 3.7 wt%, the yield strength was slightly increased to 240.1 MPa, while the elongation was further reduced to 1.01%. Further increasing the Ni content to 4.7 wt%, the yield strength was increased to 262.8 MPa, while the elongation was maintained

at similar level of 1.03%.

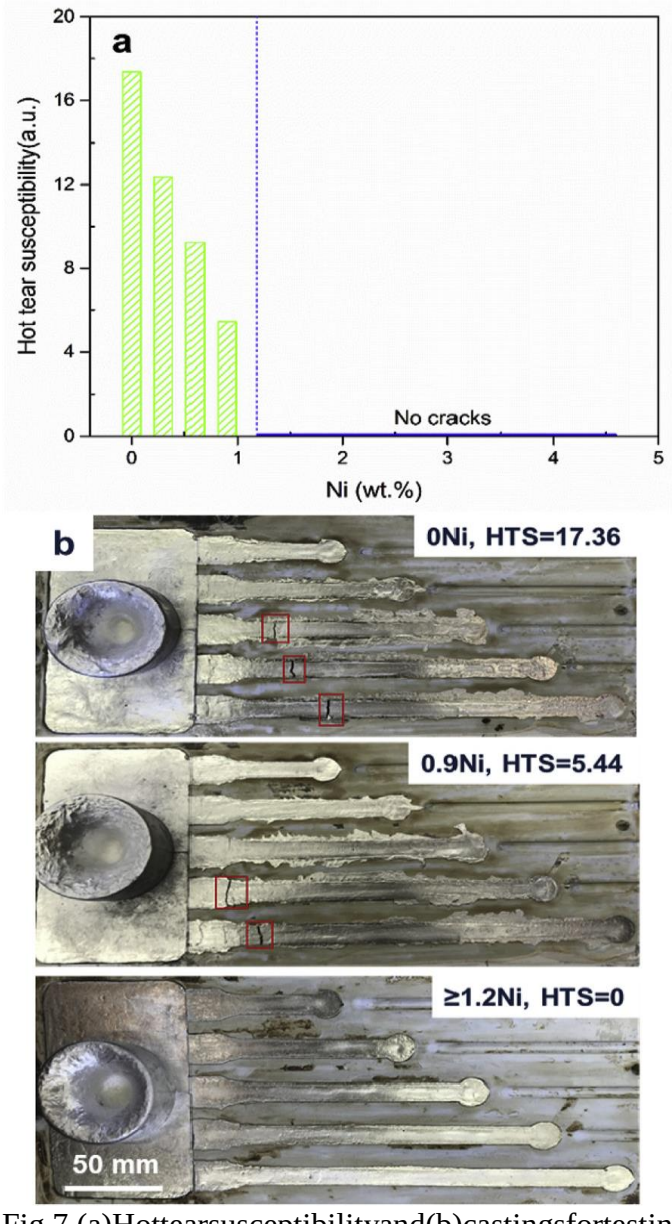


Fig.7.(a)Hottearsusceptibilityand(b)castingsfortestinghottearbeforedemoldingasafunctionofNi contentintheAleZneMgeCueNialloysevaluatedbytheN-TecHotteartestmold.

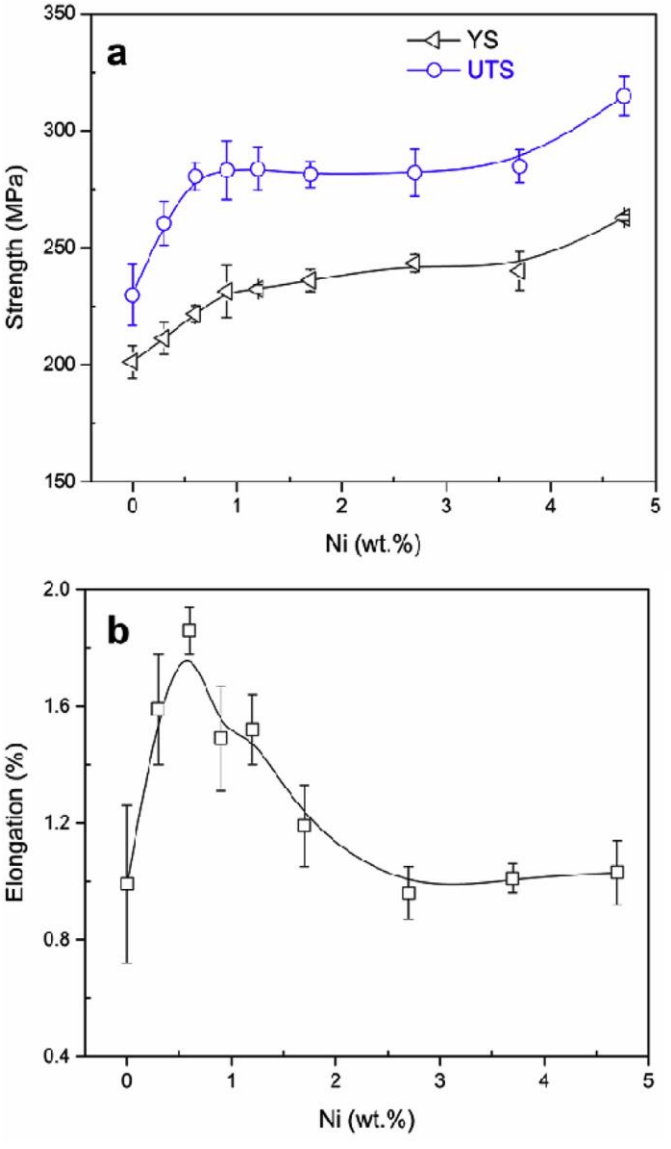


Fig.8.Mechanicalpropertiesoftheas-castAleZneMgeCueNialloysatroomtemperature,(a) ultimate tensile strength and yield strength, (b)elongation

.

4. Discussion

4.1. Solidification of AleZneMgeCueNi alloys

In order to understand the effect of Ni on solidification and microstructural evolution, CALPHAD modelling of the experimental AleZneMgeCueNi alloys was conducted using Pandat software. The Ti and other minor elements were not taken into account in calculation. The calculated equilibrium phase diagram of AleZneMgeCueNi system on the cross section of the Al-6 wt.%Zn1.4 wt%Mg-1.2 wt% Cu is shown in Fig. 9. Meanwhile, to have a better understanding of the solidification process of the experimental alloys, the phase fraction versus temperature of several typical experimental alloys was also calculated and shown in Fig. 10a.

According to Fig. 9, the calculated equilibrium phase can be divided into several regions according to different solidification behaviour with different Ni contents. The phase formation via liquid-solid reactions in the alloys are as follow:

(1) when Ni < 0.18 wt%, only one liquid-solid reaction L/Lþa-AlP occurred.

(2) when 0.18 wt% < Ni content < 4.34 wt%, L/Lþa-AlP/aAlPþ(a-Al þ Al3Ni)E.

(3) when Ni > 4.34 wt%, L/L þ Al3NiP/Al3NiPþ(a-Al þ Al3Ni)E with prior Al3Ni phase.

The subscript P referred to the primary phase and E referred to the eutectics. After the liquid-solid reactions, the Al2CuMg phase, MgZn2 phase and Al3Cu5Zn2 phase are sequentially precipitated in all the experimental alloys via solid-solid reactions. And it is also noted that the initial formation temperatures of the intermetallic phases including Al3Ni, Al2CuMg, MgZn2 and Al3Cu5Zn2 have a small increase with increasing the Ni content (shown in Figs. 9 and 10a).

According to Fig. 10a, it is found that although the mole fraction of MgZn2,Al2CuMg and Al3Cu5Zn2 phases are different during solidification, but they are very close at 100 $^{0}$C. While, the Al3Ni phase fractions of different alloys always have a significant difference during the solidification process. The strengthening effect of different phases is closely related with that are from the final phase fractions in solidified alloys. There, the phase fraction (at 100 $^{0}$C) in the all experimental Al-6 wt.%Zn-1.4 wt%Mg-1.2 wt% Cu alloys with different Ni contents is calculated and illustrated in Fig. 10b. It is found that the addition of Ni only increases the mole fraction of Al3Ni phase but almost has no obvious influence on the mole fractions of MgZn2,Al2CuMg and Al3Cu5Zn2 phase. According to the CALPHAD results in Fig. 10b, the phase fractions of Al2CuMg and Al3Cu5Zn2 are only 0.8 mol.% and 0.6 mol.%, respectively. Therefore, their effect on strengthening is limited at such a low fraction. The main strengthening phase is MgZn2, and its phase fraction has a very small increase with the increase of Ni content, which changes from 4.02 mol.% in the Ni-free alloy to 4.16 mol.% in the alloy with
4.7 wt%Ni. Meanwhile, as the Ni content increases from 0 to 4.7 wt %, the phase fraction of Al3Ni can reach 9.9 mol.%. As such, Al3Ni becomes the dominant strengthening phase, resulting in a great influence on the mechanical properties of the experimental alloys.

However, it needs to emphasize that the equilibrium Al3Cu5Zn2 phase was not observed in the as-cast microstructures of the experimental AleZneMgeCu-xNi alloys, and also the equilibrium primary Al3Ni phase was rarely identified in the alloy containing
4.7 wt% Ni. The differences can be attributed to several factors including the variation of the actual non-equilibrium solidification in gravity casting process and the accuracy of the database used in the equilibrium phase diagram calculation. It was also reported previously that Al3Cu5Zn2 was not identified in AleZneMgeCu based alloys for its very low fraction

and also it may be mixed with other intermetallic phases [27e30].

One interesting phenomenon was also noticed in the present work. According to the phase diagram, both the h-MgZn2 and SeAl2CuMg phases precipitated by solid-solid reactions from Al matrix. While, from Figs. 2 and 3, the irregular h-MgZn2 phase was

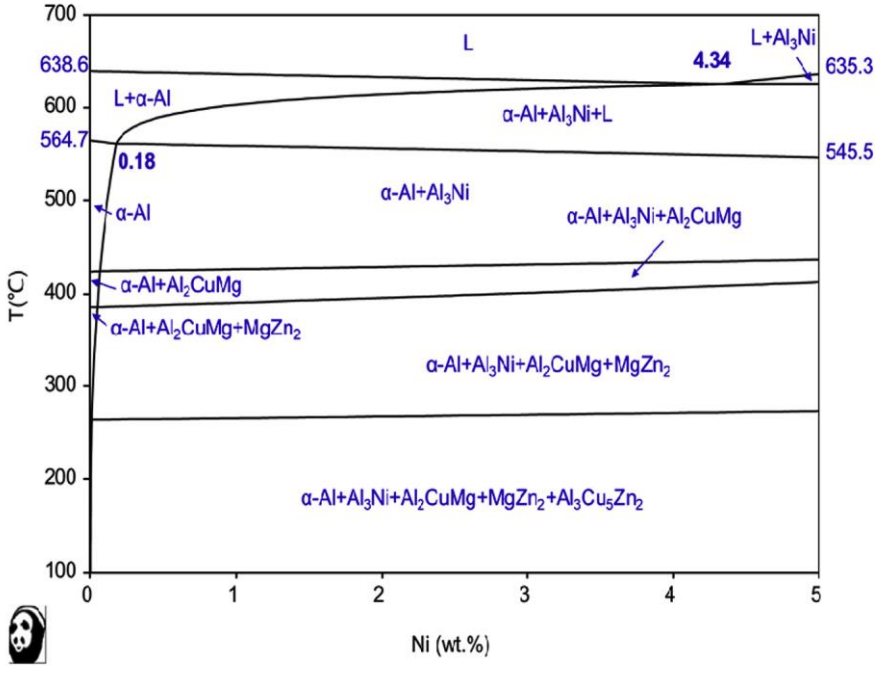


Fig. 9. The equilibrium phase diagram of AleZneMgeCueNi system on the cross section of the Al-6 wt.%Zn-1.4 wt%Mg-1.2 wt% Cu calculated using Pandat software.

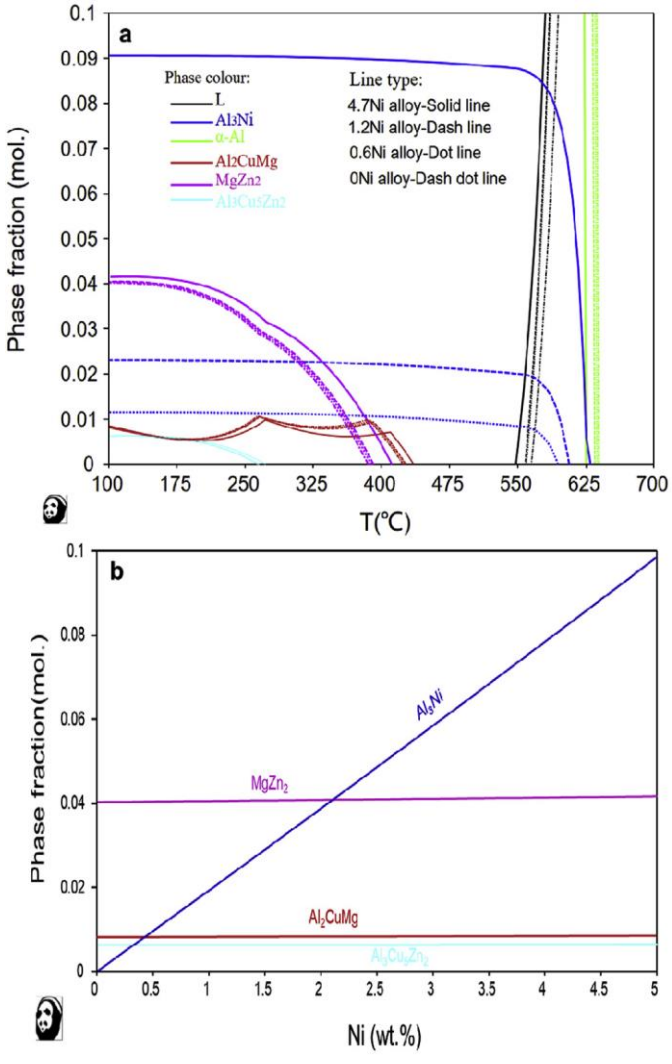


Fig.10.Phasefractionversustemperature(100e7000C)(a)and(b)phasefraction(at1000C)oftheAl-6wt.%Zn-1.4wt%Mg-1.2wt%CuwithdifferentNicontentscalculatedusingPandatsoftware.

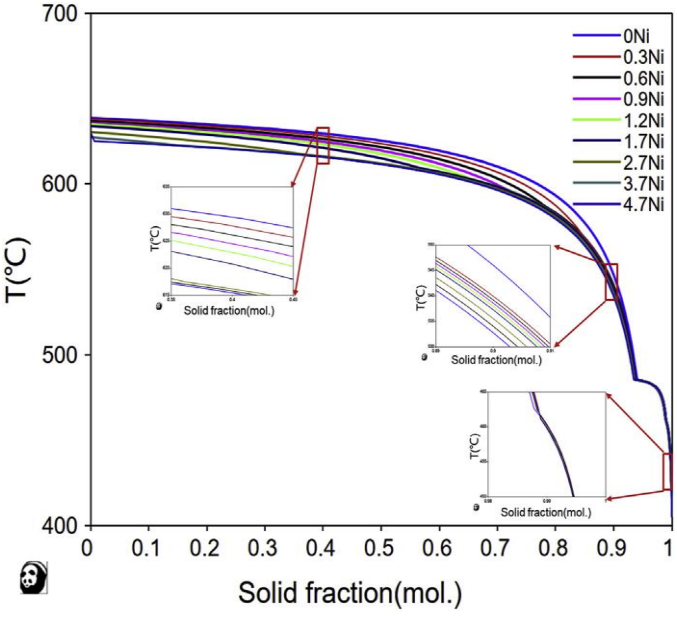


Fig.11.CalculatedtemperatureatdifferentsolidfractionsforAle6Zn-1.4Mg-1.2Cu-xNialloysusin gPandatsoftware.

mainly distributed at the grain boundary, but SeAl2CuMg phase formed in the a-Al grains and had a round shape as shown in Fig. 5. Considering all atoms forming h-MgZn2 and SeAl2CuMg phases are from Al solid solution, the interesting difference in distribution locations of these two phases should be determined by the different mobility of solute atoms in a-Al matrix. While, a further study is still needed to describe the details. It has been reported that the diffusion coefficient of Zn, Mg and Cu in Al matrix are 4.9 x $10^{-12}$ $m^2$/s, 6.2 x $10^{-12}$ $m^2$/s and 1.8 x $10^{-12}$ $m^2$/s, respectively [47]. Therefore, it can be concluded that Cu hindered the long-range diffusion of precursor of SeAl2CuMg phase and forced it precipitate in Al matrix. While, a further study is still needed to describe the detail. As for Al3Ni phase, it precipitated from melt directly according to the phase diagram, thus would be pushed to the grain boundary areas during the following solidification process.

4.2. The mechanism of improving hot tear resistance

To understand the hot tear behaviour, experimental methods combined with hot tear criteria would be a suitable approach. Initially, the freezing range (FR) is used to evaluate the tendency to hot tear. Usually, the wider FR is, the higher tendency to hot tear is. However, many researchers have reported that this criterion is not well consistent with the actual hot tear experimental results [23,28,29,48e50]. Therefore, researchers have adopted other criteria to evaluate the HTS index. Clyne and Davies developed a HTS index based on the concept of vulnerable time period versus the time available for accommodation [48]. The HTS index was named as the cracking susceptibility coefficient (CSC) as follow:

CSC ¼ tV/tR (2)

Where tV is the time during solidification in which the casting is vulnerable to cracking, usually tV ¼ t0.99-t0.9, and tR is the time available for the stress relief process, usually tR ¼ t0.9-t0.4.

Generally, there is no tendency to hot tear when the solid fraction is at 0.4e0.9, while the hot tear would occur if the solidification time is too long when the solid fraction is increased from 0.90 to 0.99. And when the solid fraction is above 0.99, the alloys will be too strong to hot tear. For the convenience of calculation, the time can be replaced by the temperature at the corresponding solid fraction [49,50] based on the consideration of the same average cooling rate, and so the TV and CSC* ¼ (T0.9-T0.99)/(T0.4-T0.9)are usually used to evaluate the tendency to hot tear.

In order to analyze the mechanism of improving hot tear resistance of AleZneMgeCu alloys with different Ni contents, the theoretical calculation of temperature at different solid fractions for all the experimental alloys was calculated, and the results are listed in Fig. 11 and Table 2. It is found that the finishing temperatures of solidification (solid fraction ¼ 0.99) of all the experimental alloys are almost the same, but the temperatures with solid fraction of 0.4 and 0.9 are obviously different. It is seen that the TV and CSC* values are gradually reduced with increasing the Ni content, which is well agreed with the experimental results. Therefore, the CSC model can well describe the effect of Ni content on the HTS of the experimental AleZneMgeCueNi alloys.

To further understand the improvement in hot tear resistance, the fracture was examined in the failure alloy and the results are depicted in Figs. 12 and 13, respectively. It can be seen that the alloy without Ni had a relatively flat fracture surface (Fig. 12), and smooth a-Al grains and several dot-like intermetallics were observed. Several ruptured liquid films were also clearly observed on the fractured surface. During solidification, a-Al dendrites are usually formed as prior phase and the interconnected network is

Table 2
Calculated temperature at different solid fractions with Scheil model for Ale6Zn-1.4Mg-1.2Cu-xNi alloys using Pandat software.

| Ni content (wt.%) | Tl ($^0$C) | Ts($^0$C) | FR($^0$C) | T0.4 ($^0$C) | T0.9 ($^0$C) | T0.99 ($^0$C) | TV($^0$C) | CSC* |
|---|---|---|---|---|---|---|---|---|
| 0 | 638.62 | 564.66 | 73.96 | 629.43 | 546.08 | 460.02 | 86.06 | 1.033 |
| 0.3 | 637.65 | 559.63 | 78.02 | 627.6 | 539.94 | 460.4 | 79.54 | 0.907 |
| 0.6 | 636.7 | 557.95 | 78.75 | 626.34 | 539.19 | 460.35 | 78.84 | 0.904 |
| 1. | 635.74 | 556.57 | 79.17 | 625.5 | 538.57 | 460.32 | 78.25 | 0.900 |
| 2. | 634.79 | 555.45 | 79.34 | 624.89 | 537.94 | 460.27 | 77.67 | 0.893 |

1. 633.53 553.85 79.68 624.57 537.27 459.69 77.58 0.889
2. 630.38 548.54 81.84 622.17 535.57 460.05 75.52 0.872
3. 627.21 544.99 82.22 620.76 534.05 459.87 74.18 0.855
4. 629.4 542.46 86.94 618.43 532.55 459.72 72.83 0.848

Note: Tl is liquidus temperature, Ts is solidus temperature, FR is freezing range, FR ¼ Tl-TsTV ¼ T0.9-T0.99, CSC*¼(T0.9-T0.99)/(T0.4-T0.9)[49,50].

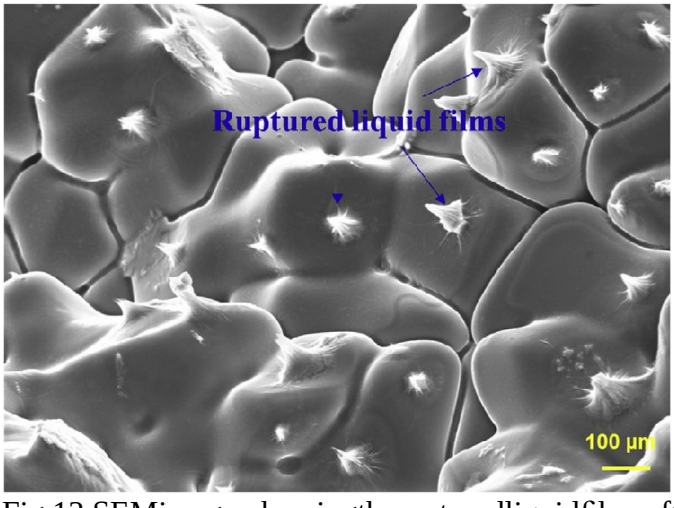

Fig.12.SEMimagesshowingtherupturedliquidfilmsofthehottearsurfaceinalloywithout Ni.

formed after growth. In the same time, a small amount of liquid is still existed in the form of film in the small gap among the arm space of solid a-Al dendrites. Meanwhile, the thermal strain and ,T0.4,T0.9 and T0.99 are the temperature of 0.4, 0.9 and 0.99 solid fraction, respectively, stress formed during solidification also accumulated and played on the liquid film, making the liquid film become thinner and thinner.

Once the thermal stress is larger than the strength of remaining liquid film, the liquid film is ruptured and hot tear is initiated. From the diagram shown in Fig. 9, all the melt is precipitated as primary a-Al phase. In other words, there was no eutectic melt exist between a-Al phase therefore can’trefill the initial cracks. As the result, the initial tear would propagate quickly and induced the hot tear finally.

From Fig. 13, it can be found that the Ni-containing alloys possessed a bumpy fractured surface with numerous bright dendritic intermetallic phases among the primary a-Al dendrites (Fig. 13 b, c, d), which were identified as the Al3Ni phase. When the Ni content is climbed from 0.3 wt% to 0.9 wt%, the mole fraction of eutectic Al3Ni phase is obviously increased. According to the CALPHAD results, Al3Ni is formed via a eutectic reaction L/(a-Al þ Al3Ni)E at the last stage of solidification after the precipitation of primary a-Al via the reaction L/Lþa-AlP. Therefore, the increased Al3Ni phase on the fractured surface means that

the remnant liquid among the solid primary a-Al dendrites becomes more and more. In this case, the initial tears would be refilled by the sufficient remaining eutectic liquid. Thus, the HTS significantly is reduced with further increasing Ni content due to the increment in the amount of eutectic liquid. In other words, the higher the content of remaining liquid, the less likely the hot tear is initiated, due to large amount of liquid available to block the propagation of the crack.

Therefore, the decrease of TV and CSC*, and the increase of eutectic Al3Ni phase content are the main reasons for the improvement in the hot tear resistance of the experimental alloys.

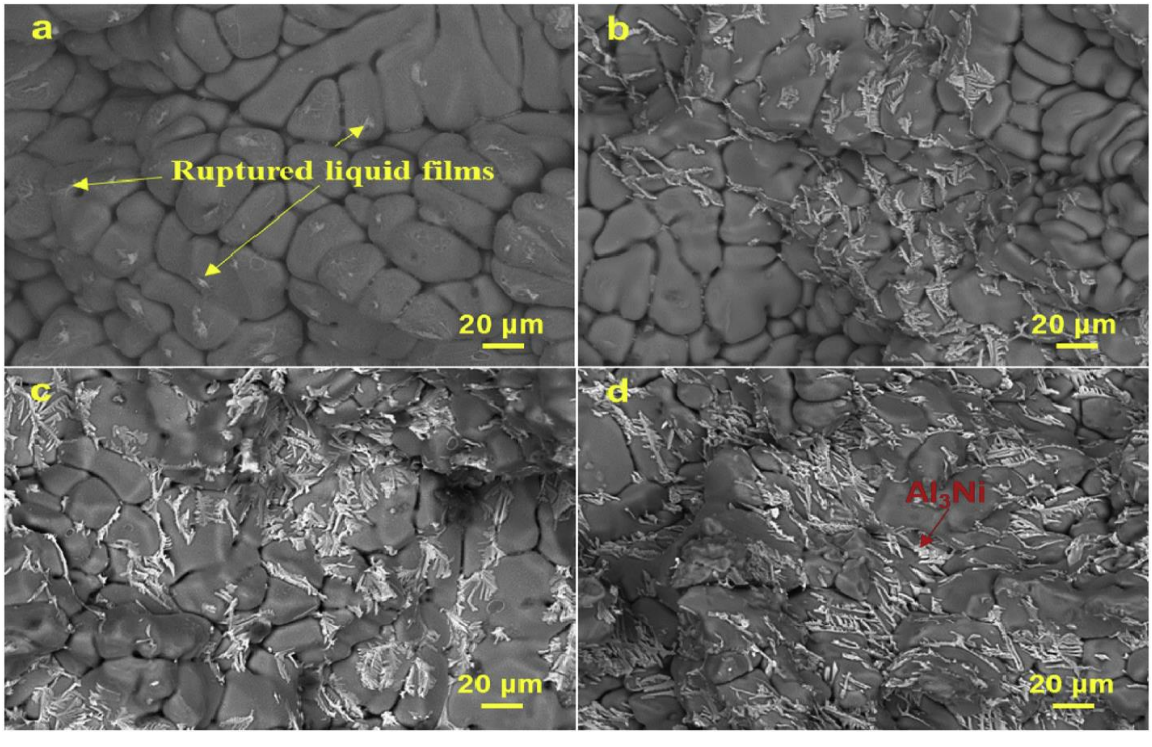


Fig. 13. Backscatter SEM fractography images showing the hot tear surface of AleZneMgeCueNi alloys, (a) 0Ni, (b) 0.3Ni, (c) 0.6Ni and (d) 0.9Ni.

4.3. Fractured surface and the microstructure-properties relationship

The mechanical properties of the experimental alloys are closely related to their as-cast microstructures, including matrix, strengthening phases as well as defects. To further investigate the underlying mechanism of the mechanical properties variation in experimental alloys, the fractured surfaces after tensile testing at room temperature were analyzed and the results are exhibited in Fig. 14.

From Fig. 14 a and b, it is found that many separated a-Al grain boundaries appeared on the fractured surface of the Ni-free alloy. It means that there exists a lots of initial shrinkage

porosities between a-Al grains, which can be also observed from Fig. 2. As discussed above, the shrinkage porosity is induced by the sufficient remaining eutectic liquid, and then results in a high hot tear tendency. For the mechanical properties, the shrinkage porosity also plays a negative role. During tensile test, the porosities would be the initial part of crack and result in low strength and elongation simultaneously. From Fig. 14b, it can be found the dimples on the fracture surface of the Ni-free alloy is small and shadow, which is the feature of unfavored ductility.

In the Ni-containing alloys, Al3Ni phase is formed and acted as strengthening phase due to its high values of Young's modulus (116e152 GPa), hardness (HV0.01 ¼ 5130 MPa) and tensile strength (2160 MPa) [35,36], while the rigid Al3Ni compound is substantially inert in the alloy and acts as hard pinning points restraining dislocation motion which can affect the strength and elongation of Al alloys. Meanwhile, according to the discussion above, the amount of eutectic melt would increase, thus the initial shrinkage porosity can be refilled and healed. Therefore, the amount of shrinkage porosities in castings decreased obviously. As the result, the separated a-Al grain boundaries on the fractured surface of Nicontaining alloys become less and are even disappeared, as shown in Fig. 14 c-h. On the other hand, Ni addition (0e0.6 wt%) also refines a-Al grains continually (Fig. 4). The improvements on shrinkage defects and grain size could increase both the strength and the elongation simultaneously. It should be mentioned that although the strengthening phase Al3Ni has a deleterious effect on elongation, the elongation increment from the defect improvement and refinement is more obvious, therefore both the elongation and strength could be improved as Ni content is increased from 0 to 0.6 wt%, as shown in Fig. 8.

As Ni content further increased from 0.6 wt% to 2.7 wt%, it still has a small grain refinement (Figs. 3 and 4), and the hard Al3Ni phase content is increased continually. The combined effect of refinement and Al3Ni phase hardening result in the improvement of strength and the decrease of elongation. And when the Ni content changed from 2.7 wt% to 4.7 wt%, the elongation is kept at the same level with the increment of strength, which may be caused by the shape variation and aggregation of the strengthening Al3Ni phase (shown in Figs. 2e5), and it needs to point out that the dendritic Al3Ni phases can link together to form integral hard points leading to great improvement in strength of the alloy with wt%Ni.

## Conclusions

In the present paper, the effects of Ni content on the phase formation, microstructural evolution, hot tear susceptibility and mechanical properties of the Al-6 wt.% Zn-1.4 wt%Mg-1.2 wt%Cu alloy produced by gravity casting were investigated, and the main results

were concluded as follows:

(1) In the experimental AleZneMgeCueNi alloys under as-cast condition, there are four phases including a-Al matrix, hMgZn2,SeAl2CuMg and Al3Ni phases. The round SeAl2CuMg phase is distributed in a-Al matrix, and the other intermetallic phases are mainly at grain boundaries. The addition of Ni increases the phase fraction of Al3Ni but has no effect on the phase formation of h-MgZn2 and SeAl2CuMg.

(2) The addition of Ni decreases TV and CSC*. Therefore, it is favorable for the improvement in hot tear resistance. When Ni content is greater than 1.2 wt%, the experimental alloys have no tendency to hot tear.

(3) The strength and elongation of experimental AleZneMgeCueNi alloys are improved simultaneously when Ni addition is less than 0.6 wt% due to the effects of Ni on healing initial tears, refinement, forming Al3Ni phase for strengthening. While, when Ni content is more than 0.6 wt%, the strength is increased but the elongation is decreased.

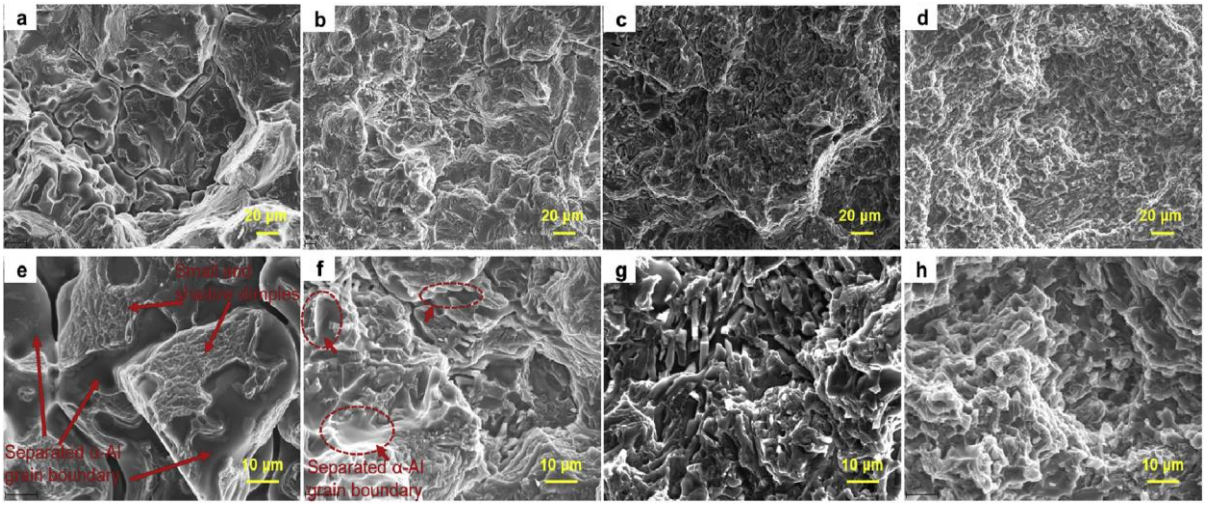


Fig. 14. Typical SEM images showing fractured surface of the as-cast AleZneMgeCueNi alloys after tensile test, (a,e)0Ni, (b,f)0.6Ni, (c,g)1.7Ni and (d,h)4.7Ni.

Acknowledgements

Financial support from Innovate UK under project 11019 is gratefully acknowledged.

References

[1] X. Zhang, Y. Chen, J. Hu, Recent advances in the development of aerospace materials, Prog. Aerosp. Sci. 97 (2018) 22e34.

[2] S. Ji, D. Watson, Z. Fan, M. White, Development of a super ductile diecast AleMgeSi alloy, Mater. Sci. Eng., A 556 (2012) 824e833.

[3] S. Ji, D. Watson, Y. Wang, M. White, Z. Fan, Effect of Ti addition on mechanical

properties of high pressure die cast Al-Mg-Si alloys, in: Materials Science Forum, vol 765, Trans Tech Publ, 2013, pp. 23e27.

[4] P. Rambabu, N.E. Prasad, V.V. Kutumbarao, R. Wanhill, Aluminium alloys for aerospace applications, in: Aerospace Materials and Material Technologies, 2017, pp. 29e52.

[5] W.S. Miller, L. Zhuang, J. Bottema, A.J. Wittebrood, P.D. Smet, A. Haszler,

A. Vieregge, Recent development in aluminium alloys for the automotive industry, Mater. Sci. Eng., A 280 (2000) 37e49.

[6] R. Ghiaasiaan, B.S. Amirkhiz, S. Shankar, Quantitative metallography of precipitating and secondary phases after strengthening treatment of net shaped casting of Al-Zn-Mg-Cu (7000) alloys, Mater. Sci. Eng., A 698 (2017) 206e217.

[7] R. Ghiaasiaan, S. Shankar, Effect of alloy composition on microstructure and tensile Properties of net-Shaped castings of AleZneMgeCu alloys, Int. J. Metalcast. 13 (2019) 300e310.

[8] X. Li, Q. Cai, B. Zhao, Y. Xiao, B. Li, Effect of nano TiN/Ti refiner addition content on the microstructure and properties of as-cast Al-Zn-Mg-Cu alloy, J. Alloy. Comp. 675 (2016) 201e210.

[9] X. Yan , J. C. Lin, C. Yanar, L. Zellman, X. Dumant, R. Tombari, E. Lafontaine, Al-Zn-Mg-Cu-Sc High Strength Alloy for Aerospace and Automotive Castings, U.S. Patent, (2012) No. 8157932.

[10] G.D. Janaki Ram, T.K. Mitra, V. Shankar, S. Sundaresan, Microstructural refinement through inoculation of type 7020 AleZneMg alloy welds and its effect on hot cracking and tensile properties, J. Mater. Process. Technol. 142 (2003) 174e181.

[11] Y. Li, Z. Zhang, Z. Zhao, H. Li, L. Katgerman, J. Zhang, L. Zhuang, Effect of main elements (Zn, Mg, and Cu) on hot tearing susceptibility during direct-chill casting of 7xxx aluminum alloys, Metall. Mater. Trans. A 50 (2019) 3603e3616.

[12] M. Yildirim, D. Ozyürek, M. Gürü, The effects of precipitate size on the hardness and wear behaviors of aged 7075 aluminum alloys produced by powder metallurgy route, Arabian J. Sci. Eng. 41 (2016) 4273e4281.

[13] J. Dutkiewicz, H.V. Atkinson, L. Litynnska, T. Czeppe, M. Modigell, nska-DobrzynCharacterization of semi-solid processing of aluminium alloy 7075 with Sc and Zr additions, Mater. Sci. Eng., A 580 (2013) 362e373.

[14] C. Xu, J. Zhao, A. Guo, H. Li, G. Dai, X. Zhang, Effects of injection velocity on microstructure, porosity and mechanical properties of a rheo-diecast Al-Zn-Mg-Cu aluminum alloy, J. Mater. Process. Technol. 249 (2017) 167e171.

[15] W. Zhu, W. Mao, Q. Wei, C. Hui, Y. Shi, Preparation of Al-Zn-Mg-Cu alloy semisolid slurry through a water-cooled serpentine pouring channel, China Foundry 16 (2019) 31e39.

[16] G. Gan, C. Zhang, D. Yang, M. Yang, X. Jiang, Y. Shi, Effect of TiB2 on micro-

structure of 7075 Al alloy semi-solid slurry at different solid fraction, Mater. Trans. 58 (2017) 734e738.

[17] L. Litynnska, P. Ochin, A. Gnnska-Dobrzynoral, M. Faryna, J. Dutkiewicz, The microstructure of rapidly solidified Al-Zn-Mg-Cu alloys with Zr addition, in: Solid State Phenomena, vol 163, Trans Tech Publ, 2010, pp. 42e45.

[18] H. Yu, M. Wang, Y. Jia, Z. Xiao, C. Chen, Q. Lei, Z. Li, W. Chen, H. Zhang, Y. Wang, High strength and large ductility in spray-deposited AleZneMgeCu alloys, J. Alloy. Comp. 601 (2014) 120e125.

[19] H. Li, F. Cao, S. Guo, Y. Jia, D. Zhang, Z. Liu, P. Wang, S. Scudino, J. Sun, Effects of Mg and Cu on microstructures and properties of spray-deposited Al-Zn-Mg-Cu alloys, J. Alloy. Comp. 719 (2017) 89e96.

[20] J. Dong, J. Cui, F. Yu, Z. Zhao, Y. Zhuo, A new way to cast high-alloyed AleZneMgeCueZr for super-high strength and toughness, J. Mater. Process. Technol. 171 (2006) 399e404.

[21] J. Dong, Z. Zhao, J. Cui, F. Yu, C. Ban, Effect of low-frequency electromagnetic casting on the castability, microstructure, and tensile properties of direct-chill cast Al-Zn-Mg-Cu alloy, Metall. Mater. Trans. A 35 (2004) 2487e2494.

[22] S.Y. Park, W.J. Kim, Enhanced hot workability and post-hot deformation microstructure of the as-cast Al-Zn-Cu-Mg Alloy fabricated by use of a high-frequency electromagnetic casting with electromagnetic stirring, Metall. Mater. Trans. A 48 (2017) 3523e3539.

[23] Q. Bai, Y. Li, H. Li, Q. Du, J. Zhang, L. Zhuang, Roles of alloy composition and grain refinement on hot tearing susceptibility of 7xxx aluminum alloys, Metall. Mater. Trans. A 47 (2016) 4080e4091.

[24] D. Warrington, D.G. McCartney, Hot-cracking in aluminium alloys 7050 and 7010da comparative study, Cast Metals 3 (1990) 202e208.

[25] W.K. Krajewski, A.L. Greer, J. Burans, G. Piwowarski, P.K. Krajewski, New developments of high-zinc Al-Zn-Cu-Mn cast alloys, Mater. Today: Proc. 10 (2019) 306e311.

[26] S.S. Shin, K.M. Lim, I.M. Park, Characteristics and microstructure of newly designed AleZn-based alloys for the die-casting process, J. Alloy. Comp. 671 (2016) 517e526.

[27] S.S. Ebrahimi, J. Aghazadeh, K. Dehghani, M. Emamy, S. Zangeneh, The effect of Al-5Ti-1B on the microstructure, hardness and tensile properties of a new Zn rich aluminium alloy, Mater. Sci. Eng., A 636 (2015) 421e429.

[28] S. Lin, C. Aliravci, M.O. Pekguleryuz, Hot-tear susceptibility of aluminum wrought alloys and the effect of grain refining, Metall. Mater. Trans. A 38 (2007) 1056e1068.

[29] J. Shin, T. Kim, D. Kim, D. Kim, K. Kim, Castability and mechanical properties of new 7xxx aluminum alloys for automotive chassis/body applications, J. Alloy. Comp. 698 (2017) 577e590.

[30] G. Rajaram, S. Kumaran, T.S. Rao, Effect of graphite and transition elements (Cu, Ni) on high temperature tensile behaviour of AleSi Alloys, Mater. Chem. Phys. 128 (2011) 62e69.

[31] L. Lattanzi, M. Di Giovanni, M. Giovagnoli, A. Fortini, M. Merlin, D. Casari, M. Di Sabatino, E. Cerri, G. Garagnani, Room temperature mechanical properties of A356 alloy with Ni additions from 0.5 wt to 2 wt%, Metals 8 (2018) 1e15.

[32] Z. Asghar, G. Requena, F. Kubel, The role of Ni and Fe aluminides on the elevated temperature strength of an AlSi12 alloy, Mater. Sci. Eng., A 527 (2010) 5691e5698.

[33] D. Casari, T.H. Ludwig, M. Merlin, L. Arnberg, G.L. Garagnani, The effect of Ni and V trace elements on the mechanical properties of A356 aluminium foundry alloy in as-cast and T6 heat treated conditions, Mater. Sci. Eng., A 610 (2014) 414e426.

[34] H. Yang, D. Watson, Y. Wang, S. Ji, Effect of nickel on the microstructure and mechanical property of die-cast AleMgeSieMn alloy, J. Mater. Sci. 49 (2014) 8412e8422.

[35] J. Hernandez-Sandoval, G.H. Garza-Elizondo, A.M. Samuel, S. Valtiierra,

F.H. Samuel, The ambient and high temperature deformation behavior of AleSieCueMg alloy with minor Ti, Zr, Ni additions, Mater. Des. 58 (2014) 89e101.

[36] H.T. Naeem, K.S. Mohammed, K.R. Ahmad, A. Rahmat, The influence of nickel and tin additives on the microstructural and mechanical properties of Al-Zn-Mg-Cu Alloys, Adv. Mater. Sci. Eng. 2014 (2014) 1e10.

[37] N.A. Belov, Quantitative phase analysis of the Al-Zn-Mg-Cu-Ni phase diagram in the region of compositions of high-strength nickalines, Russ. J. Non-Ferrous Metals 51 (2010) 243e249.

[38] T.K. Akopyan, N.A. Belov, A.N. Alabin, G.S. Zlobin, Calculation-experimental Study of the Aging of Casting High-Strength Al-Zn-Mg-(Cu)-Ni-Fe Aluminum Alloys, Russian Metallurgy (Metally), 2014, pp. 60e65, 2014.

[39] T.K. Akopyan, A.G. Padalko, N.A. Belov, Z.A. Karpova, Effect of Barothermal Treatment on the Structure and the Mechanical Properties of a High-Strength Eutectic AleZneMgeCueNi Aluminum Alloy, Russian Metallurgy (Metally), 2017, pp. 922e927, 2017.

[40] ASTM standard: B108 (2003a), Standard Specification for Aluminum-Alloy Permanent Mold Castings, ASTM International, 2003, pp. 1e15.

[41] X. Dong, Y. Zhang, S. Amirkhanlou, S. Ji, High performance gravity cast Al9Si0.45Mg0.4Cu alloy inoculated with AlB2 and TiB2, J. Mater. Process. Technol. 252 (2018) 604e611.

[42] T. Koutsoukis, M.M. Makhlouf, Alternatives to the AleSi eutectic system in aluminum casting alloys, Int. J. Metalcast. 10 (2016) 342e347.

[43] J.R. Davis, ASM Specialty Handbook, Aluminum and Aluminum Alloys, ASM international Handbook Committee, Materials Park, OH, 1993.

[44] W. Yang, S. Ji, X. Zhou, I. Stone, G. Scamans, G.E. Thompson, Z. Fan, Heterogeneous

nucleation of a-Al grain on primary a-AlFeMnSi intermetallic investigated using 3D SEM ultramicrotomy and HRTEM, Metall. Mater. Trans. A 45 (2014) 3971e3980.

[45] C. Suwanpreecha, P. Pandee, U. Patakham, C. Limmaneevichitr, New generation of eutectic Al-Ni casting alloys for elevated temperature services, Mater. Sci. Eng., A 709 (2018) 46e54.

[46] C. Li, Y. Wu, H. Li, Y. Wu, X. Liu, Effect of Ni on eutectic structural evolution in [49] N. Hatami, R. Babaei, M. Dadashzadeh, P. Davami, Modeling of hot tearing hypereutectic AleMg2Si cast alloys, Mater. Sci. Eng., A 528 (2010) 573e577. formation during solidification, J. Mater. Process. Technol. 205 (2008)

[47] G. Neumann, C. Tuijn, Self-diffusion and Impurity Diffusion in Pure Metals: 506e513. Handbook of Experimental Data, Elsevier, 2011. [50] J. Liu, S. Kou, Crack susceptibility of binary aluminum alloys during solidifi

[48] T.W. Clyne, G.J. Davies, Influence of composition on solidification cracking cation, Acta Mater. 110 (2016) 84e94. susceptibility in binary alloy systems, Br. Foundryman 74 (1981) 65e73.